

Sl. No.	<p style="text-align: center;">IIT Ropar List of Recent Publications with Abstract Coverage: December, 2019</p>
1.	<p>A note on generalizations of Stieltjes constants T Chatterjee, SS Khurana - Journal of the Ramanujan Mathematical Society, 2019</p> <p>Abstract: In this article we consider a generalization of Stieltjes constants and study its relation with special values of certain Dirichlet series. Further we show a connection of these constants with a generalization of Digamma function. Some of the results obtained are a natural generalization of the identities of Gauss, Lehmer, Dilcher and many other authors.</p>
2.	<p>A Review on Voltage and Frequency Control of Micro Hydro System PS Bhakar, S Sarangi, K Gupta - Intelligent Computing Techniques for Smart Energy Systems - Part of the Lecture Notes in Electrical Engineering book series (LNEE, volume 607), 2020</p> <p>Abstract: Modern technology developed in renewables has opened a door to utilize micro hydro as one of the major sources of energy in micro-grid in terms of capital investment and sustainability. With such developments, frequency and voltage variation in micro-grid arise as a major concern where conventional control technique fails. This has driven the idea to develop electronic load controller to dump extra power hence minimizing the frequency variations. As the efficiency is reduced using such methods, batteries are applied in micro hydro to store the dumped power. However, to improve both voltage and frequency, combination of ELC and STATCOM are developed. Further, in order to improve the system performance, modifications in ELC corresponding to the load configuration were developed and proved to be beneficial. To improve the efficiency of the system, water heaters, pump loads, or other low wattage apparatus are also used. This paper presents a survey on various frequency and voltage control techniques available in small hydro system with their merits and demerits. The investigations on various problems demand further development.</p>
3.	<p>Anticipating critical transitions in epithelial–hybrid–mesenchymal cell-fate determination S Sarkar, SK Sinha, H Levine, MK Jolly, PS Dutta - Proceedings of the National Academic Sciences of the USA, 2019</p> <p>Abstract: In the vicinity of a tipping point, critical transitions occur when small changes in an input condition cause sudden, large, and often irreversible changes in the state of a system. Many natural systems ranging from ecosystems to molecular biosystems are known to exhibit critical transitions in their response to stochastic perturbations. In diseases, an early prediction of upcoming critical transitions from a healthy to a disease state by using early-warning signals is of prime interest due to potential application in forecasting disease onset. Here, we analyze cell-fate transitions between different phenotypes (epithelial, hybrid-epithelial/mesenchymal [E/M], and mesenchymal states) that are implicated in cancer metastasis and chemoresistance. These transitions are mediated by a mutually inhibitory feedback loop—microRNA-200/ZEB—driven by the levels of transcription factor SNAIL. We find that the proximity to tipping points enabling these transitions among different phenotypes can be captured by critical slowing down-based early-warning signals, calculated from the trajectory of ZEB messenger RNA level. Further, the basin stability analysis reveals the unexpectedly large basin of attraction for a hybrid-E/M phenotype. Finally, we identified mechanisms that can potentially elude the transition to a hybrid-E/M phenotype. Overall, our results unravel the early-warning signals that can be used to anticipate upcoming epithelial–hybrid–mesenchymal transitions. With the emerging evidence about the hybrid-E/M phenotype being a key driver of metastasis, drug resistance, and tumor</p>

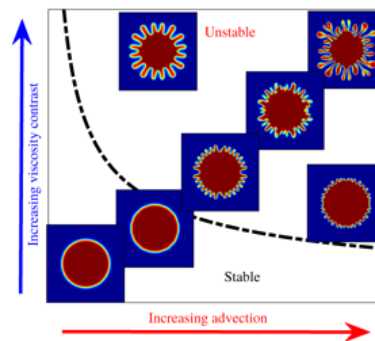
relapse, our results suggest ways to potentially evade these transitions, reducing the fitness of cancer cells and restricting tumor aggressiveness.

[Control of radial miscible viscous fingering](#)

V Sharma, S Nand, S Pramanik, CY Chen, M Mishra - *Journal of Fluid Mechanics*, 2019

4.

Abstract: We investigate the stability of radial viscous fingering (VF) in miscible fluids. We show that the instability is determined by an interplay between advection and diffusion during the initial stages of flow. Using linear stability analysis and nonlinear simulations, we demonstrate that this competition is a function of the radius r_0 of the circular region initially occupied by the less-viscous fluid in the porous medium. For each r_0 , we further determine the stability in terms of Péclet number (Pe) and log-mobility ratio (M). The Pe - M parameter space is divided into stable and unstable zones: the boundary between the two zones is well approximated by $\alpha M c = \alpha(r_0) Pec - 0.55$. In the unstable zone, the instability is reduced with an increase in r_0 . Thus, a natural control measure for miscible radial VF in terms of r_0 is established. Finally, the results are validated by performing experiments that provide good qualitative agreement with our numerical study. Implications for observations in oil recovery and other fingering instabilities are discussed.

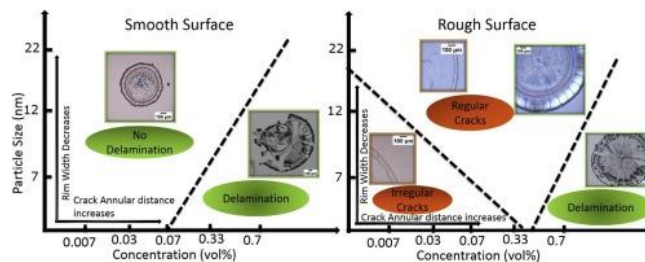


[Coupled effect of concentration, particle size and substrate morphology on the formation of coffee rings](#)

D Lohani, MG Basavaraj, DK Satapathy, S Sarkar - *Colloids and Surfaces A : Physicochemical and Engineering Aspects*, 2019

5.

Abstract: Our study reports the coupled effects of particle size, concentration and the substrate roughness on the evaporation process of an aqueous sessile droplet containing silica nanoparticles. The patterns formed after complete drying of the sessile drops have also been studied. On smooth substrates the droplets evaporate in constant contact angle (CCA) and mixed modes (MM) with CCA mode as the predominant mode of evaporation. For substrates with nanoscale roughness all the three, namely CCA, constant contact radius (CCR) and MM modes exist with CCR mode as the predominant mode of evaporation. On nanorough substrates, droplets leave circular ring-shaped stains due to strong pinning along the droplet perimeter whereas irregular shape stains are formed on smooth substrates. We found that the rim width of the ring-like particulate deposits scales with the particle concentration following a power law behavior. Furthermore, we compared crack density and uniformity of cracks in the deposits formed on both substrates obtained by drying aqueous drops containing particles of different sizes and concentrations. For a given roughness, delamination is found to occur in the deposits formed by drying drops with higher particle concentration and smaller particle size. Finally, we summarize our study by presenting a phase diagram to classify the particulate deposits and the crack patterns as a function of particle concentration and substrate roughness.

Graphical Abstract:

[Donor Acceptor Cyclopropanes as an Expedient Building Block Towards the Construction of N-Containing Molecules: Recent Update](#)

P Singh, RK Varshnaya, R Dey, P Banerjee - *Advanced Synthesis & Catalysis*, 2019

6.

Abstract: Nitrogen-containing molecules are the key structural constituent of many pharmaceutical compounds that play a pivotal role in drug development. Owing to their multifaceted medicinal importance, several synthetic approaches have been delineated in the recent past for their construction. Over the past few decades the augmented use of donor-acceptor cyclopropanes (DACs) as three carbon synthetic equivalent despite their ring strain, for the construction of innumerable hetero- and carbocycles of pharmaceutical importance have raised interests of synthetic chemists towards it. Owing to their zwitterionic nature due to the vicinal disposition of donor and acceptor groups, they have been frequently used in ring-opening reactions, cycloadditions, and rearrangements. This review is mainly focused on assorted reactions of DACs with various nitrogen-containing dipolarophiles like imines, azides, cyanates, isothiocyanates, nitrosocarbonyls, hydrazines, diaziridines, triazinanes, diazenes, etc. towards the synthesis of nitrogen-containing molecules of pharmaceutical and industrial importance. This review is in continuation of our review published in the *Israel Journal of Chemistry* in April 2016, including the literature from April 2016 to May 2019.

[Drone Assisted Network Coded Co-operation](#)

P Kumar, P Singh, S Darshi, S Shailendra - *2019 IEEE Region 10 Conference (TENCON)*, 2019

7.

Abstract: In this paper, we propose Drone Assisted Network Coded Co-operation (DA-NCC) for next generation wireless networks to achieve good quality of service, better spectral efficiency and improved diversity. Unlike typical cooperative networks, DA-NCC makes use of drone as a relay node which provides additional degree of freedom in terms of movement. By adjusting the vertical position of drone, probability of getting Line of Sight component for Source (S)-Relay (R) and Relay (R)-Destination (D) links may be improved. For accurate characterization of such networks, Rayleigh faded channel for Source (S)-Destination (D) pair and probability based mixture model of Rayleigh and Rician faded channels for S-R and R-D pair are considered. Analytical expressions for network coded noise, variance of network coded noise, signal to overall noise ratio at destination node and rate are derived and verified through monte carlo simulation. Our investigation reveals that use of drone improves the network performance. However, drone height needs to be determined scrupulously. Such drone assisted communication set-up may play an important role in disaster management scenarios where communication through infrastructured base station is disrupted due to natural calamities.

8.

[Energy Production Through Gasification of Waste Biomass in Punjab Region](#)

R Goswami, S Verma, R Das - *Emerging Trends in Mechanical Engineering - Part of the Lecture Notes in Mechanical Engineering book series (LNME)*, 2020

	<p>Abstract: This paper presents useful energy (gas and power) production from the three waste biomass (dried grass, leaves, and dead branches) through gasification technology. These waste biomasses were collected in the Indian Institute of Technology Ropar, Punjab and air-dried. The feasibility of the studied biomass for thermochemical conversion process in a downdraft biomass gasifier has been investigated by characterization of biomass. The average higher heating values based on the ultimate and proximate analysis correlation were evaluated as 15.58 MJ/kg for dried grass, 17.075 MJ/kg for leaves and 15.785 MJ/kg for dead branches. The performance of downdraft biomass gasifier has been investigated in terms of calorific value (3.52 MJ/m³ for dried grass, 5.14 MJ/m³ for leaves and 4.15 MJ/m³ for dead branches) and cold gas efficiency (50.83%, for dried grass, 64.72% for leaves and 59.15% for dead branches). The results show that these waste biomass are a reliable source for energy production through gasification technology having dual benefits of easy waste management and low-cost power production.</p>
9.	<p>Exotic origins of tensionless superstrings A Bagchi, A Banerjee, S Chakraborty, P Parekh - Physics Letters B, 2019</p> <p>Abstract: A new type of tensionless superstring theory, called the Inhomogeneous tensionless superstring, has been recently introduced. This is characterised by a residual symmetry algebra on the worldsheet richer in structure than the previously known symmetry algebra related to Homogeneous tensionless superstring. In this paper, we investigate theories of tensile superstring that the Inhomogeneous tensionless superstring with manifestly real fermions could arise from. We provide two different candidates for these parent tensile theories. The nature of the limit dictates that these theories have some exotic features.</p>
10.	<p>Exploration of highly selective fluorogenic 'on-off'chemosensor for H₂PO₄⁻ ions: ICT-based sensing and ATPase activity profiling YB Wagh, KC Tayade, A Kuwar, SK Sahoo, N Singh... - Luminescence, 2019</p> <p>Abstract: In this study, the recognition contour of Chemosensor 1 was investigated using semiaqueous methanol (XH, mole fraction = 0.31) for a range of anions and bioactive species. Host-receptor signalling based on the internal charge transfer mechanism for Chemosensor 1 was explored and reported. Structure of Chemosensor 1 and its plausible anion coordination based on hydrogen bonding is complemented with density functional theory. Consequently, we investigated the applicability of the synthesized probe in blood plasma, urine, tap water samples, and for monitoring of ATP in lysosomes by apyrase enzyme.</p>
11.	<p>Feasibility Demonstration of μEDM for Fabrication of Arrayed Micro Pin-fins of Complex Cross-sections H Kishore, CK Nirala, A Agrawal - Manufacturing Letters, 2020</p> <p>Abstract: Thermal management in microelectronics components through micro pin-fins heat sinks is well understood. This work aims to propose an unexplored methodology for fabrication of such MPFs having cross-sections in shapes of droplet, aerofoil, piranha and diamond of dimensions as less as 200 μm and height up to 1200 μm. Density of these pin-fins has been achieved more than 4 pins/mm² on brass plates. The methodology is basically a retrieval of μEDM which has been combined with LASER micromachining to achieve the goal. Research directions for possible improvement in 'quality of the pin-fins' and 'material removal rate' have been proposed at the end.</p>
12.	<p>Flat-top laser beams over an extended range ANK Reddy, V Pal, S Mahler, AA Friesem, N Davidson - Journal of Physics: Conference Series, 2019</p>

	<p>Abstract: Designs based on single diffractive-optical-elements for obtaining flat-top laser intensity distributions that remain constant over a long range during free-space propagation are presented. Flat-top beams with different orders n exhibit a different range of propagation. For various working distances z, the resulting flat-top beam yields a different depth of focus. By controlling spectral properties of laser distributions, it is possible to maintain invariant flat-top intensity distributions for relatively long propagation distances.</p>
13.	<p><u>Formation of Au/Au₉Ga₄ Alloy Nanoshell on Bacterial Surface through Galvanic Displacement Reaction for High-Contrast Imaging</u> A Singh, D Bains, WM Hassen, N Singh, JJ Dubowski - ACS Applied Bio Materials, 2019</p> <p>Abstract: The spontaneous electron transfer between GaAs and ionic gold through the galvanic displacement reaction results in formation of gold nanoparticles and Au₉Ga₄ alloy. We investigated this process for decorating Legionella pneumophila and Escherichia coli aiming at enhanced imaging of these bacteria. The surface of bacteria was modified with gold ions through the electrostatic linkage of ionic liquids with phosphate units of the bacterial cell wall. The modified bacteria were further incubated with antibody-functionalized GaAs substrate. Due to a large gap in the reduction potential of gold and gallium ions, the induced reaction involving bacteria resulted in a reduction of the gold ions to gold nanoparticles and oxidation of GaAs to Ga₂O₃ and Au₉Ga₄ alloy. The bacteria covered with an Au/AuGa nanoshell, if excited at 377 nm, show a bright emission at 447 nm originating from Au/Au₉Ga₄. This approach offers a simple and potentially less expensive method for high-contrast imaging of bacteria in comparison to the conventional methods of staining with different dyes or by conjugating green fluorescent proteins.</p>
14.	<p><u>Generation of non-classical states of photons from a metal–dielectric interface: a novel architecture for quantum information processing</u> K Mehta, VG Achanta, S Dasgupta - Nanoscale, 2020</p> <p>Abstract: We show the possibility to generate photons in a certain class of non-classical states from a metal–dielectric interface using dipole emitters on the interface. The photons emitted into the surface plasmon mode from the initially excited emitters radiate out in free space in a cone-shaped geometry. When detected at two detectors, these photons exhibit coalescence, a clear signature of non-classicality. Such a system can also be employed as a building block for a distributed quantum network. We further show that it is indeed feasible to implement our model using available technology.</p>
15.	<p><u>How Smart Are Smart Classrooms? A Review of Smart Classroom Technologies</u> MK Saini, N Goel - ACM Computing Surveys (CSUR), 2019</p> <p>Abstract: There has been a large amount of work on smart classrooms spanning over a wide range of research areas including information communication technology, machine learning, sensor networks, mobile computing, and hardware. Consequently, there have been several disparate reviews on various aspects of smart classrooms. Such piecemeal development is not sufficient for a pragmatic smart classroom solution. This article complements the literature by providing a consolidated review of interdisciplinary works under a common nomenclature and taxonomy. This multi-field review has exposed new research opportunities and challenges that need to be addressed for the synergistic integration of interdisciplinary works.</p>

[Lifetime measurements of phosphorus isotopes using the AGATA \$\gamma\$ -ray tracking spectrometer](#)
L Grocutt, R Chapman, M Bouhelal, F Haas, A Goasduff...PP Singh... - Physical Review C, 2019

16.

Abstract: Lifetimes of excited states of the phosphorus isotopes $^{33,34,35,36}\text{P}$ have been measured by using the differential recoil-distance method. The isotopes of phosphorus were populated in binary grazing reactions initiated by a beam of ^{36}S ions of energy 225 MeV incident on a thin ^{208}Pb target mounted in the Cologne plunger apparatus. The combination of the PRISMA magnetic spectrometer and an early implementation of the AGATA γ -ray tracking array was used to detect γ rays in coincidence with projectile-like nuclear species. Lifetime measurements of populated states were made within the range from about 1 to 100 ps. The number of states for which lifetime measurements were possible was limited by statistics. For ^{33}P , lifetime limits were determined for the first $3/2^+$ and $5/2^+$ states at 1431 and 1848 keV, respectively; the results are compared with previous published lifetime values. The lifetime of the first 2^+ state of ^{34}P at 429 keV was determined and compared with earlier measurements. For ^{35}P , the states for which lifetimes, or lifetime limits, were determined were those at 2386, 3860, 4101, and 4493 keV, with $J\pi$ values of $3/2^+$, $5/2^+$, $7/2^-$, and $7/2^-$, respectively. There have been no previous published lifetimes for states in this nucleus. A lifetime was measured for the stretched $\pi(1f7/2)\otimes\nu(1f7/2)J\pi=(7^+)$ state of ^{36}P at 5212 keV and a lifetime limit was established for the stretched $\pi(1d3/2)\otimes\nu(1f7/2)J\pi=(5^-)$ state at 2030 keV. There are no previously published lifetimes for states of ^{36}P . Measured lifetime values were compared with the results of state-of-the-art shell-model calculations based on the PSDPF effective interaction. In addition, measured branching ratios, published mixing ratios, and electromagnetic transition rates, where available, have been compared with shell-model values. In general, there is good agreement between experiment and the shell model; however there is evidence that the shell-model values of the M1 transition rates for the $3/2^+ \rightarrow 1/2^+$ (ground state) and $5/2^+ \rightarrow 3/2^+$ transitions in ^{33}P underestimate the experimental values by a factor between 5 and 10. In ^{35}P there are some disagreements between experimental and shell-model values of branching ratios for the first and second excited $7/2^-$ states. In particular, there is a serious disagreement for the decay characteristics of the second $7/2^-$ state at 4493 keV, for which the shell-model counterpart lies at 4754 keV. In this case, the shell-model competing electromagnetic decay branches are dominated by E1 and M1 transitions.

[Microstructural investigations on bonding mechanisms of cold-sprayed copper with SS316L steel](#)

S Singh, H Singh, RK Buddu - Surface Engineering, 2019

17.

Abstract: The purpose of the study was to understand the adhesion mechanism between cold-sprayed copper and SS316L steel substrate. Coatings of 3-mm thickness were deposited by cold-spraying on steel substrates prepared with different roughness values. To understand the bonding mechanism of the coating with substrates, scanning electron microscopy (SEM), and energy dispersive spectroscopy (EDS) analyses were done on interfacial surfaces; exposed after the adhesion testing. Additionally, cross-sectional as-well-as top surface deformation behaviour of single copper particles deposited on steel substrates was investigated by using SEM/EDS, to elucidate the mechanism behind bonding. The results of the study validated that the adhesion is governed by both metallurgical bonding, as-well-as, mechanical interlocking, owing to the jetting formation. The mirror-polished surface resulted in a better adhesion strength as compared to the as-received and semi-polished surfaces, which was further validated by ultrasonic testing. Also, smaller-sized particles were found to be favourable for good adhesion strength.

18.	<p>Mitochondria-and nucleolus-targeted copper (I) complexes with pyrazole-linked triphenylphosphine moieties for live cell imaging R Rani, A Singh, N Garg, N Kaur, N Singh - Analyst, 2020</p> <p>Abstract: The labelling and imaging of mitochondria and nucleolus have attracted great attention because of the involvement of these cellular organelles in critical cellular activities. Therefore, a large number of mitochondria- or nucleolus-labelling probes have been developed throughout the world. However, in the current study, we successfully developed two pyrazole-based, copper-linked triphenylphosphine-coupled emissive metallo-complexes (C1 and C2) for the simultaneous visualization of mitochondria and nucleolus in a single run. These complexes were very inexpensive and could be synthesized by a simple one-pot multicomponent reaction scheme. The complexes were very specific, and only a small concentration of 5 μM was found to be sufficient to probe both the organelles efficiently. Additionally, even under a shorter incubation period (half hour), the fluorescence intensity from the cells was appreciable. Also, both the compounds were found to be photostable when torched with 10% of a 100 mW laser for up to 10 min. All these results indicate that both the complexes may contribute towards the future development of cell imaging tools. To the best of our knowledge, this is the first report on the development of multifunctional live cell imaging tools for simultaneous mitochondria and nucleolus imaging and within the shortest incubation time of about 30 minutes.</p>
19.	<p>Molecular interpretation of mechanical behavior in four basic crystal packing of Isoniazid with homologous cocrystal formers JP Yadav, RN Yadav, P Uniyal, H Chen, C Wang...N Kumar... - Crystal Growth & Design, 2019</p> <p>Abstract: Conformation of homologous cocrystal formers (hCCFs, (HOOC—(CH₂)_n—COOH, n=1 to 6 and 8)) led to differential intermolecular interactions with Isoniazid (INZ) forming four basic molecular packing. These molecular packing are defined based on their H-bonded basic structural motifs. Their mechanical behavior was systematically evaluated using nanoindentation and correlating them to “in-die” Heckel analysis, “out-of-die” bulk compaction and stress-strain relationship. Counter-intuitively, known structural feature crystallographic slip planes exhibited relatively lower plasticity and plastic energy in INZ:SUC, and higher E, H and apparent mean yield pressure. Similar behavior was observed for isostructural crystal packing of INZ:ADP. On the other hand, superior plasticity was achieved in INZ:GLT and INZ:MLN, leading to larger bonding area. However its tabletability was lower. Conversely, stiffer molecular crystals INZ:SUC and INZ:ADP provided higher tensile strength having higher elastic modulus, mechanical hardness and apparent mean yield pressure. Despite being low symmetry molecular solids, substantial correlation was found with anticipation that preferred orientation of molecular planes provides close approximation of their bulk compression and consolidation behavior. This study demonstrated that molecular level crystal structure governs linkage between particle level nanomechanical attributes and bulk level deformation behavior.</p>
20.	<p>Near perfect thin film flexible broadband optical absorber with high thermal/electrical conductivity V Ghai, H Singh, PK Agnihotri - Journal of Applied Polymer Science, 2019</p> <p>Abstract: Flexible ultra-black absorber with high thermal/electrical conductivity finds huge applications in the field of stray light attenuation, solar collectors, flexible electronics, and electronic thermal management systems. In this work, we report the fabrication of ultrablack absorber consists of vertically aligned carbon nanotubes (VACNT) in Polydimethylsiloxane</p>

	<p>(PDMS) having an absorption capacity of more than 98% in UV–Vis wavelength and more than 94% in NIR wavelength range. It is observed that the PDMS-VACNT composite shows ultra-high absorption capacity due to enhanced impedance matching and multiple scattering. In addition to this, the PDMS-VACNT composite shows an emissivity of 0.94 along with a 118% increase in thermal conductivity. Moreover, with the infiltration of VACNT in PDMS, the sheet resistance decrease drastically to 0.08 KΩ/sq, which signify the possible use of ultrablack absorber in electronic skin and flexible sensors etc.</p>
21.	<p>Performance of RC Frame Base-Isolated Building with Geotextile as Isolator Using UPBD Method AK Chaudhary, S Choudhury - Journal of The Institution of Engineers (India): Series A, 2019</p> <p>Abstract: In the present paper, the RC-framed fixed-base buildings are compared with the RC-framed base-isolated buildings using the geotextile as an isolator. As the cost of the traditional isolators is much higher, emphasis is given here to test the friction isolator by modelling RC-framed buildings using SAP 2000. The values used for the friction isolator were determined in the laboratory test using actuator which were found to be 42,000 kN/m, and average coefficient of friction was 0.67. The present study is aimed at ascertaining the applicability of the unified performance-based design (UPBD) method in carrying out design for performance level in displacement-based design of RC-framed buildings and comparatively study the performances of the RC-framed buildings with fixed-base building and base-isolated buildings using UPBD method. The performance parameters have been evaluated by performing nonlinear time history analysis for RC-framed buildings with fixed-base and base-isolated for mid-rise buildings.</p>
22.	<p>Prophylactic potential of cytolethal distending toxin B (CdtB) subunit of typhoid toxin against Typhoid fever R Thakur, P Pathania, N Kaur, V Joshi, KK Kondepudi, RC Suri... - Scientific Reports, 2019</p> <p>Abstract: Typhoid fever caused by Salmonella enterica serovar Typhi (S.Typhi) continues to be a major problem, especially in developing countries. Due to the rapid emergence of multi-drug-resistant (MDR) strains, which limits the efficacy of conventional antibiotics as well as problems associated with the existing vaccines, efforts are being made to develop effective prophylactic agents. CdtB subunit of typhoid toxin was selected for assessing its vaccine potential due to its high conservation throughout the Typhi strains. In-vitro assessment of DNase activity of cloned and purified CdtB protein showed a significant decrease in the band intensity of DNA. The measure of metabolic activity and morphological alterations assessed using different cell lines in the presence of CdtB protein showed no significant signs of toxicity. These observations were further strengthened by cell cycle analysis, assessed by flow cytometry. Keeping these observations in mind, the immunoprotective potential of CdtB was assessed using S.Typhi induced mouse peritonitis model. A significant titer of IgG antibodies (>128000) against CdtB protein was recorded in the immunized mice by enzyme-linked immunosorbent assay (ELISA), which was also validated by immunoblotting. Active immunization with the protein protected 75% mice against a lethal dose of S.Typhi Ty2. The data indicated a significant (up to 5 log) reduction in the bacterial load in the spleen and liver of immunized-infected mice compared to control (unimmunized-infected) mice which might have resulted in the modulation of histoarchitecture of spleen and liver and the levels of cytokines (IL-6, TNF-α and IL-10) production; thereby indicating the effectiveness of the subunit. The observations deduced from the study give the proof of concept of immunogenic potential of protein. However, further studies involving the immunoreactivity of CdtB with the statistically significant number of sera samples obtained from the human patients would be helpful in establishing the relevance of</p>

	CdtB protein in humans and for making the strategies to develop it as an effective vaccine candidate.
23.	<p>Quantification of carbon nanotube dispersion and its correlation with mechanical and thermal properties of epoxy nanocomposites M Tiwari, BK Billing, HS Bedi, PK Agnihotri - Journal of Applied Polymer Science, 2019</p> <p>Abstract: An experimental study is carried out to quantitatively assess the dispersion quality of carbon nanotubes (CNTs) in epoxy matrix as a function of CNT variant and weight fraction. To this end, two weight fractions (0.05% and 0.25%) of as-grown, oxidized, and functionalized CNTs are used to process CNT/epoxy nanocomposites. Scanning electron microscopy, X-ray diffraction, and Fourier transform infrared analysis of different variants of CNTs are used to establish the efficiency of purification route. While the relative change in mechanical properties is investigated through tensile and micro-hardness testing, thermal conductivity of different nanocomposites is measured to characterize the effect of CNT addition on the average thermal properties of epoxy. Later on, a quantitative analysis is carried out to establish the relationship between the observed improvements in average composite properties with the dispersion quality of CNTs in epoxy. It is shown that carboxylic (-COOH) functionalization reduces the average CNT agglomerate size and thus ensures better dispersion of CNTs in epoxy even at higher CNT weight fraction. The improved dispersion leads to enhanced interfacial interaction at the CNT/epoxy interface and hence provides higher relative improvement in nanocomposite properties compared to the samples prepared using as-grown and oxidized CNTs.</p>
24.	<p>Torque Ripple Minimization with Maximum Utilization of Inductance Profile in 6/4 3-Phase Switched Reluctance Motor Drives AK Rana, AVR Teja - 45th Annual Conference of the IEEE Industrial Electronics Society, 2019</p> <p>Abstract: This paper presents a novel method to fully utilize the positive slope region of SRM phase inductance profile and generate a maximum positive torque while simultaneously reducing the torque ripple effectively. The proposed method is based on explicit mathematical model with comparatively lesser computational overhead. Using the proposed modus operandi, torque ripple could be reduced to $\leq 3\%$. The proposed algorithm is implemented on a 6/4 3-Phase SRM using Matlab/Simulink and the results are reported.</p>

Disclaimer: This publication digest may not contain all the papers published. Library has compiled the publication data as per the alerts received from Scopus and Google Scholar for the affiliation “Indian Institute of Technology Ropar” for the month of December 2019. The author(s) are requested to share their missing paper(s) details if any, for the inclusion in the next publication digest.